Double-Pendulum Tower Crane Trolley Trajectory Planning: A Parameter Based Time-Polynomial Optimization

Shichen Sun[1,2], Juhao Su[1,2], Yu Hin Ng[2], Ching-Wei Chang[2]

[1]Academy of Interdisciplinary Studies, The Hong Kong University of Science and Technology, Hong Kong S.A.R.
[2]Hong Kong Center for Construction Robotics, Hong Kong S.A.R.

ssunbb@connect.ust.hk, jsuan@connect.ust.hk, sampsonng@ust.hk, ccw@ust.hk

Abstract -

Modeling the tower crane as a double pendulum dynamic system introduces complexities in control considerations. To tackle this challenge, this paper presents a time-polynomial-based trajectory generation method. This method enables the reconstruction of direct commands and employs high-order fitting to align with various control constraints. The differential solutions of the swing angles, obtained from the linearized dynamic equations, can be minimized as the trolley completes its movement. Additionally, the trajectory is optimized based on time considerations to ensure the most efficient path while adhering to the safety limitations of the tower crane. With the proposed method, the trajectory curve of the trolley is a high-order polynomial with all the coefficients related to the system parameters, which makes the trajectory applicable against the change in the system parameters. Based on the trolley actuator output, the function of the swing angles could be derived as the feedback reference line to make the proposed control method robust against external disturbance. The efficacy of the proposed method is validated through real-scale simulations and compared to existing approaches, including linear quadratic regulator (LQR) and another published CTP method, demonstrating its good control performance.

Keywords -

Tower crane; Double pendulum; Time-based polynomial; Trajectory planning

1 Introduction

With the ongoing transformation and advancement of the construction industry, the utilization of Modular Integrated Construction (MiC) is steadily growing. MiC's factory-based prefabrication has streamlined on-site construction processes, enhanced construction efficiency and promoted standardized construction practices, thereby ensuring superior construction quality [1]. However, the installation sequence of prefabricated modules is predetermined [2], and their size and weight bring heightened transportation requirements at the construction site, with its expenses remaining consistently elevated [3].

Figure 1. MiC and tower crane.

Tower cranes are widely used in construction sites for transporting large-sized objects, whose slight vibrations could be capable of causing significant accidents, thereby emphasizing the importance of advanced control methods. To achieve more precise control in such scenarios, it is necessary to establish an elaborate numerical model that represents a double pendulum structure. However, the complexity of the double pendulum structure poses greater demands on the design of the controller [4].

Over the past decades, numerous control theories have been proposed to regulate tower crane transportation and reduce angle swing. Feedback control systems, such as model predictive control [5], [6], sliding mode control [4], [7], [8], adaptive control [9], [10], neural network control [11], [12], and neural network control have shown effectiveness in mitigating external disturbances. However, the double pendulum tower crane system could be approximately modeled as the combination of two unidirectional systems, characterized as two single input multiple output models. However, it is challenging to achieve coupling control effects across multiple outputs. Especially in real-scale models, the magnitude of displacement command changes is significantly greater than that of angle changes. Since the feedback compensations are calculated based on the differences between the desired states and actual states, the proportions of compensation are supposed to be small for positioning and large for angles. However, when the position of the trolley is close to the desired position, the small gain for the trolley error makes the positioning difficult.

Comparatively, open-loop control systems, including techniques like smooth shaping [13], input shaping [14], and trajectory planning [15], may exhibit lower robustness to external disturbances. However, these control methods consider the motor's output limitations and aim to achieve the desired state through relatively smooth control signals. By incorporating the output constraints of the motor, these control systems aim to ensure the system operates within the allowed limits and reaches the desired state in a controlled manner. In addition, open-loop control methods are not dependent on feedback signals from sensors, making them immune to delays in signal reception. This is particularly advantageous for systems with multiple control considerations. The primary concern only lies in the complexity of calculating the output based on the physical model.

Recently, Li et.al [16] published a time-polynomial-based trajectory planning method for double pendulum tower cranes. After mathematical transformation, the coefficients of the trajectory polynomial are in constant form according to a scaled-down model. However, the calculation basis is the linearized equations, which would cause the superposition of error. Besides, the trajectory proposed in the study is a polynomial curve with all the coefficients as constant. Besides, the simulation only contains the situations in which the lengths and masses are little changed. The proposed polynomial trajectory is not applicable to control the real-scale system.

While previous research on tower crane control has been discussed, there are still some limitations that need to be addressed: (a) Many existing models in the literature fail to address the control of real-size tower crane double pendulums adequately. This is primarily due to the difficulty in achieving a balance with single input feedback compensation control for larger-sized models. (b) The approximate derivation of mathematics from linearized equations is less accurate and may not be applicable when there are significant changes in the system characteristics.

This article proposes a tower crane control method based on polynomial solving of differential equations. Firstly, the linearized differential equation system for controlling the swing angle of the tower crane is derived based on the physical model. Subsequently, the mathematical characteristics of the differential equation system are utilized to directly fit a polynomial of the corresponding order to reduce the errors, obtaining an appropriate motor output curve to achieve the desired control objective. Finally, through a true-size simulation model that contains saturation on trolley acceleration and velocity, the control effects of the proposed scheme on key elements are compared with those of other traditional controllers. Therefore, the following advantages are summarized:

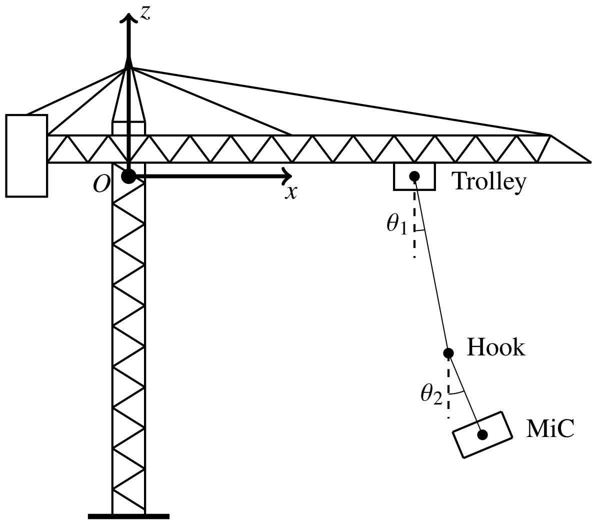

Figure 2. Depicted diagram for the model coordinate

(a) The controller exhibits good control performance for the desired endpoint state, resulting in minimal simulation error.
(b) This control method reduces the influence caused by the disparity in control weights for single-input multiple-output systems and achieves synchronous convergence control on multiple modules towards the endpoint state with the shortest time usage.
(c) This control method imposes fewer performance requirements on the motor, ensuring smooth changes in jerk, acceleration, and speed throughout the entire process, which facilitates motor control and tracking.

2 Methodology

In this research, the trajectory control derivation is started from a single-degree-of-freedom (1 DOF) tower crane. With all the objects given coordinates, the dynamics model is derived and linearized, and the trajectory of the trolley is calculated to fulfill all the control constraints.

Table 1. Tower crane parameters

Parameter	Parameter explanation	Units
M_1	Mass of the hook	kg
M_2	Mass of the payload	kg
L_1	Length of the hoisting rope	m
L_2	Length of the rigging cable	m
R	The position of the trolley	m
g	Gravity constant	m/s^2
θ_1	Hook swing angle	rad
θ_2	Payload swing angle	rad

2.1 Dynamic modeling

In Figure 2, the depicted diagram showcases the ideal setup of a 1 DOF tower crane and its associated mathematical coordinate system. Table 1 provides an overview of the pertinent parameters that define the tower crane model. The Lagrangian method is used to derive the dynamics equation from the tower crane model. As shown in Figure 2, the position vectors of the two objects are:

$$d_1 = (R + L_1\ sin\theta_1\ )\ i_x - (L_1\ cos\theta_1\ )\ i_z; \tag{1}$$

$$d_2 = (R+L_1 sin\theta_1+L_2 sin\theta_2)i_x-(L_1 cos\theta_1 + L_2 cos\theta_2)\ i_z. \tag{2}$$

The Lagrangian value (L) could be derived by the difference between kinetic energy (K_E) and potential energy (P_E), where K_E and P_E and are computed as follows:

$$K_E = \frac{1}{2}M_1 < \dot{d_1}, \dot{d_1} > +\frac{1}{2}M_2 < \dot{d_2}, \dot{d_2} >; \tag{3}$$

$$P_E = -M_1 g L_1 cos\theta_1 - M_2 g\ (L_1 cos\theta_1 + L_2 cos\theta_2)\ . \tag{4}$$

The Lagrangian equations based on the two swing angles are:

$$\frac{d}{dt}\left(\frac{\delta L}{\delta\dot{\theta_1}}\right) - \frac{\delta L}{\delta\theta_1} = 0; \tag{5}$$

$$\frac{d}{dt}\left(\frac{\delta L}{\delta\dot{\theta_2}}\right) - \frac{\delta L}{\delta\theta_2} = 0. \tag{6}$$

The simplified equations are:

$$\begin{aligned} 0 = {} & L_1(M_1 + M_2)\ddot{\theta_1} + (M_1 + M_2)\cos\theta_1\ddot{R} \\ & -(M_1 + M_2)g\sin\theta_1 + L_2 M_2\sin(\theta_1 - \theta_2)\dot{\theta_2}^2 \\ & +L_2 M_2\cos(\theta_1 - \theta_2)\ddot{\theta_2}; \end{aligned} \tag{7}$$

$$\begin{aligned} 0 = {} & L_2\ddot{\theta_2} + \cos\theta_2\ddot{R} - g\sin\theta_2 \\ & -L_1\sin(\theta_1 - \theta_2)\dot{\theta_1}^2 + L_1\cos(\theta_1 - \theta_2)\ddot{\theta_1}. \end{aligned} \tag{8}$$

The linearized dynamics equations are:

$$\begin{aligned} 0 = {} & L_1(M_1 + \ M_2)\ddot{\theta_1} + (M_1 + M_2)\ddot{R} \\ & -(M_1 + M_2)g\theta_1 + L_2 M_2\ddot{\theta_2}; \end{aligned} \tag{9}$$

$$0 = L_2\ddot{\theta_2} + \ddot{R} - g\theta_2 + L_1\ddot{\theta_1}. \tag{10}$$

2.2 Control objective

When following the command of a movement, the trolley is proposed to be controlled to the desired position. To derive the trajectory of the trolley, the initial and final target state of the trolley should satisfy the following constraints related to its jerks, accelerations, velocities, and positions:

$$R(0) = R_0;\ \dot{R}(0) = 0;\ \ddot{R}(0) = 0;\ \dddot{R}(0) = 0. \tag{11}$$

$$R(T_f) = R_d;\ \dot{R}(T_f) = 0;\ \ddot{R}(T_f) = 0;\ \dddot{R}(T_f) = 0. \tag{12}$$

where T_f is the transportation time, and R_d is the target position.

In addition, the swing angles at the end state are proposed to be controlled. The target state of the orientation of the hook and MiC should be as follows:

$$\theta_1(T_f) = 0;\ \dot{\theta_1}(T_f) = 0;\ \theta_2(T_f) = 0;\ \dot{\theta_2}(T_f) = 0. \tag{13}$$

Since the motor output has its physical limitations, during the motion, the jerk, acceleration, velocity, and position are limited under the safety values:

$$|\dddot{R}(t)| \leq J_{max};\ |\ddot{R}(t)| \leq A_{max};\ |\dot{R}(t)| \leq V_{max}. \tag{14}$$

The two angles are also limited to safety values:

$$|\theta_1(t)| \leq \theta_{1max};\ |\theta_2(t)| \leq \theta_{2max}. \tag{15}$$

2.3 Polynomial planning

The initial orientation and its derivative of the hook and MiC are listed in equations (16). The trajectory of the system is formulated as a time-polynomial with 16 coefficients as illustrated in (17), such that it has a unique solution to the 16 equations of constraint mentioned in (11), (12), (13), and (16).

$$\theta_1(0) = 0;\ \dot{\theta_1}(0) = 0;\ \theta_2(0) = 0;\ \dot{\theta_2}(0) = 0. \tag{16}$$

$$R(t) = \sum_{i=0}^{15} k_{ri}\cdot\tau^i\cdot(R_d - R_0) + R_0. \tag{17}$$

where $k_{r0},\ k_{r1},\ \ldots\ k_{r15}$ are the coefficients to be derived by the control requirements. $\tau = t/t_f$ to find the most efficient transportation time.

Substituting (11) into equation (17), we get:

$$k_{r0} = \ k_{r1} = \ k_{r2} = \ k_{r3} = 0. \tag{18}$$

For the identities (9) and (10) to hold for any time t, the coefficients of the same order of t should sum up to zero for all t orders. According to the set-up form (17), the second derivative of R has up to 13_{th} order of t, thus θ_1

and θ_2 should be formulated as time-polynomials of 13^{th} order as well as illustrated in (19) and (20), such that they can act as counter terms to eliminate the 13^{th} order terms from $\ddot{R}$.

$$\theta_1(t) = \sum_{i=0}^{13} \alpha_{ri} \cdot \tau^i, \tag{19}$$

$$\theta_2(t) = \sum_{i=0}^{13} \beta_{ri} \cdot \tau^i, \tag{20}$$

where $\alpha_0,\ \alpha_1,\ \ldots\ \alpha_{13}$ and $\beta_0,\ \beta_1,\ \ldots\ \beta_{13}$ are the coefficients to be derived from (9) and (10).

By comparing the coefficient of the 0^{th} to 13^{th} order terms in the identities (9) and (10), 14 equations are obtained from each identity, and a total of 28 equations are set for the 28 variables α and β. By rearranging the equations in terms of α and β, the 28 equations can expressed in matrix forms as follows:

$$A \cdot [\alpha_0,\ \alpha_1,\ \ldots\ ,\ \alpha_{13}, \beta_0,\ \beta_1,\ \ldots\ ,\ \beta_{13}]^T - C = 0. \tag{21}$$

where $A \in \mathbb{R}^{28\times28}$ is the coefficients matrix of α and β, and $C \in \mathbb{R}^{28\times1}$ is the constant terms from the equations.

From equation (21), the vector of variables α and β could be derived by the inverse of matrix A multiplies matrix C. $\theta_1(t)$ and $\theta_2(t)$ could thus be expressed only by the known parameters and the function $R(t)$.

After obtaining the expression of $\theta_1(t)$ and $\theta_2(t)$, 12 equations can be obtained by substituting the expressions (17) and (18) into the constraints (12), (13) and (16). The 12 equations can be expressed in matrix form as follows:

$$D(T_f,\ M_1,\ M_2,\ L_1,\ L_2,\ g) \cdot K = F. \tag{22}$$

Where $D \in \mathbb{R}^{12\times12}$ is the coefficients matrix for k_r , K is the vector of k_{r4} to k_{r15}, and $F = [1,\ 0,\ 0,\ 0,\ 0,\ 0,\ 0,\ 0,\ 0,\ 0,\ 0,\ 0]^T$.

Similarly, matrix K could be derived by the inverse of matrix D multiplies F, such that $k_{r4},\ k_{r5},\ \ldots\ k_{r15}$ are expressed only by known constant parameters and the variable T_f. The derived trajectory function $R(t)$ is simplified as:

$$R(t) = \sum_{i=4}^{15} K_{ri} \cdot \tau^i \cdot (R_d - R_0) + R_0. \tag{23}$$

where:

$K_{r4} = \frac{10810800 M_1 L_1 L_2}{(M_1+M_2) g^2 T_f^4}; K_{r5} = -\frac{121080960 M_1 L_1 L_2}{(M_1+M_2) g^2 T_f^4};$

$K_{r6} = \frac{544864320 M_1 L_1 L_2}{(M_1+M_2) g^2 T_f^4} - \frac{360360(L_1+L_2)}{g T_f^2};$

$K_{r7} = -\frac{1297296000 M_1 L_1 L_2}{(M_1+M_2) g^2 T_f^4} + \frac{2882880(L_1+L_2)}{g T_f^2};$

$K_{r8} = 6435 + \frac{1783782000 M_1 L_1 L_2}{(M_1+M_2) g^2 T_f^4} - \frac{9729720(L_1+L_2)}{g T_f^2};$

$K_{r9} = -40040 - \frac{1427025600 M_1 L_1 L_2}{(M_1+M_2) g^2 T_f^4} + \frac{18018000(L_1+L_2)}{g T_f^2};$

$K_{r10} = 108108 + \frac{618377760 M_1 L_1 L_2}{(M_1+M_2) g^2 T_f^4} - \frac{19819800(L_1+L_2)}{g T_f^2};$

$K_{r11} = -163800 - \frac{112432320 M_1 L_1 L_2}{(M_1+M_2) g^2 T_f^4} + \frac{12972960(L_1+L_2)}{g T_f^2};$

$K_{r12} = 150150 - \frac{4684680(L_1+L_2)}{g T_f^2};$

$K_{r13} = -83160 + \frac{720720(L_1+L_2)}{g T_f^2};$

$K_{r14} = 25740; K_{r15} = -3432.$

2.4 Time optimization

The minimum T_f satisfying (14) and (15) is found by the bisection method which is similar to [15]. After T_F is found, all unknowns except the time variable (t) in the trajectory function (23) are solved, and the trajectory of the trolley is fully determined while satisfying all constraints and safety limits mentioned. The polynomial function of the swing angles could also be derived.

3 Simulation

This section is conducted using Simulink in MATLAB. The section comprises two parts aimed at verifying the effectiveness of the proposed method. Section 3.1 demonstrates the accuracy of the proposed method under several situations. Section 3.2 shows the robustness of the proposed method against external disturbance. The below simulation is run with the gravitational constant $g = -9.81 m/s^2$ and a control frequency of 20Hz. The system parameters and the constraints are set as in Table 2.

Table 2. Simulation setup values

Parameter	Parameter explanation	Values
M_1	Mass of the hook	$200kg$
M_2	Mass of the payload	$1000kg$
L_1	Length of the hoisting rope	$30m$
L_2	Length of the rigging cable	$5m$
J_{max}	Upper limit of jerk	$1m/s^3$
A_{max}	Upper limit of acceleration	$0.1m/s^2$
V_{max}	Upper limit of velocity	$0.5m/s$
θ_{1max}	The upper limit of θ_1	$1deg$
θ_{2max}	The upper limit of θ_2	$1deg$

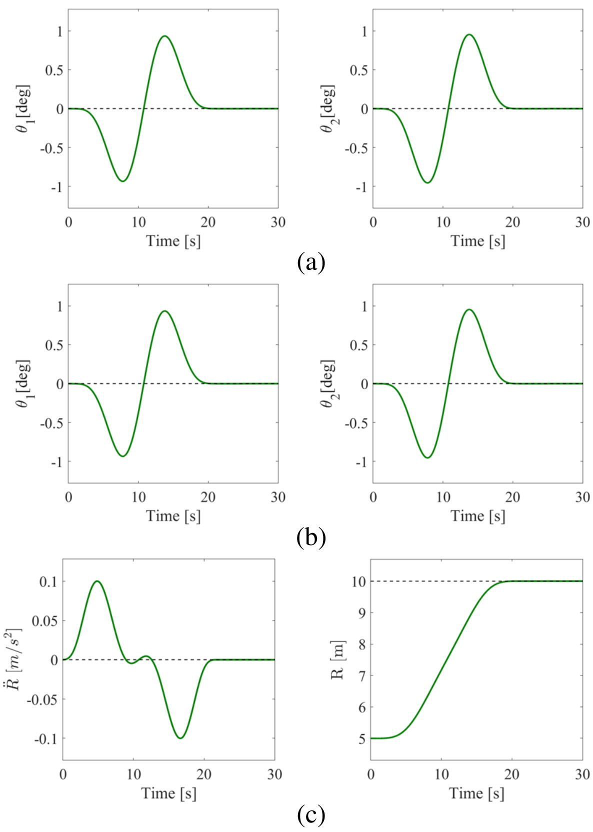

Figure 3. (a) Simulation results for the swing angle of hook (θ_1) and the payload swing angle (θ_2); (b) Theoretical values of the hook swing angle (θ_1) and the payload swing angle (θ_2); (c) The target acceleration and position of the trolley.

3.1 Accuracy verification

To prove the accuracy of the polynomial functions for trolley and swing angles, a movement command is set that the trolley moves from the position $5m$ to $10m$. The corresponding simulation results are shown in Figure 3.

Based on the figure, it can be observed that the proposed method could execute the position-changing command. The swing angles produced by the simulation environment and the ones calculated from the polynomial functions are quite similar.

3.2 Comparison controller simulation

The proposed method is also tested in the simulation environment with external disturbance. The polynomial function of the trolley and swing angles are used as feedback reference lines, and the linear quadratic regulator (LQR) is used to compensate the system errors. It is compared to the same LQR, which follows the reference lines that the angles are supposed to be zero, and composite trajectory planning (CTP) [17] methods to show the performance. The below part shows the simple derivation of LQR and the output of CTP.

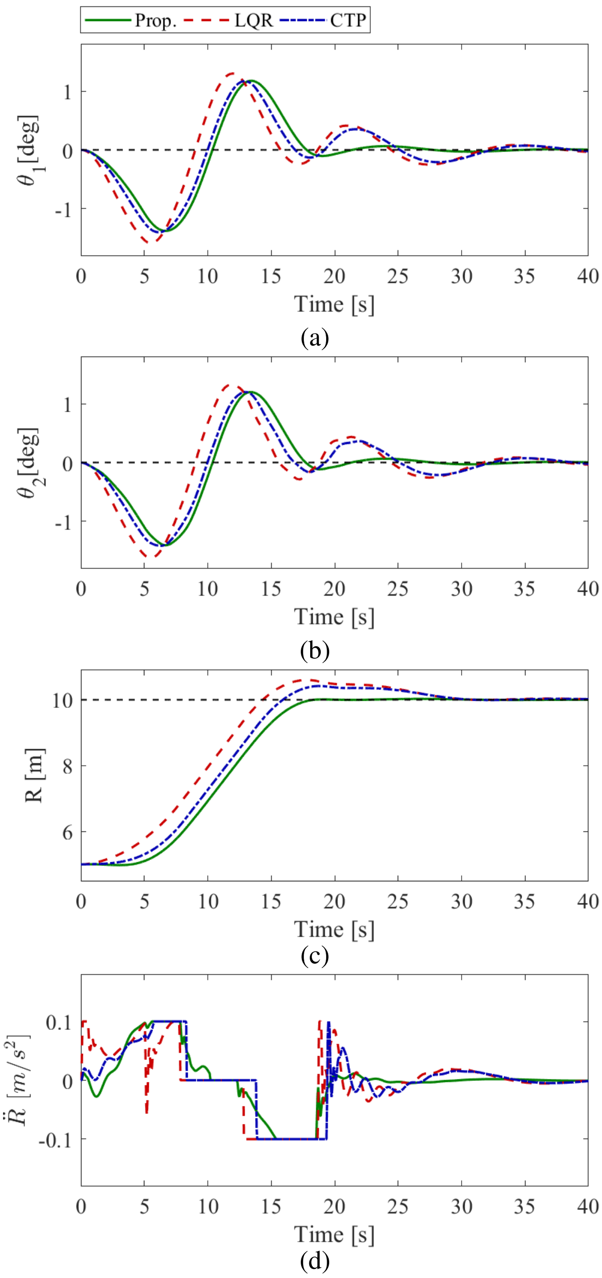

Figure 4. Simulation results for (a) the hook swing angle (θ_1), (b) the payload swing angle (θ_2), (c) the trolley position R, and (d) the trolley acceleration $\ddot{R}$ of different controllers.

Based on (9) and (10), the linearized expressions of the two angles could be derived. The state matrix of LQR is thus:

$$s = [\theta_1; \dot{\theta}_1; \theta_2; \dot{\theta}_2; R; \dot{R}]; \tag{24}$$

The cost function is:

$$J = \int_0^\infty ((s - s_{des})^T Q(s - s_{des}) + Wu^2). \qquad (25)$$

Where $u = \ddot{R}$, $Q = diag[240, 48000, 40, 8000, 5, 100]$ and $W = 1$. The gain matrix of K is calculated by MATLAB to be:

$$K = [-414.85,\ -21.95,\ 279.72,\ 17.89,\ 2.24,\ 12.89].$$

An existing CTP controller gives the output of the trolley as [17]:

$$\ddot{R} = \begin{cases} 2\pi(R_d - R_0)(sin(2\pi t/T_s))/T_s^2 \\ +k_r((M_1 + M_2)L_1\dot{\theta}_1 + M_2L_2\dot{\theta}_2),\ 0<t<T_s. \\ +k_r((M_1 + M_2)L_1\dot{\theta}_1 + M_2L_2\dot{\theta}_2), \quad t \geq T_s. \end{cases}$$

Where T_s is calculated to be $17.7s$ from the acceleration limitation.

The proposed method will use the above LQR controller to follow the polynomial lines. The LQR comparison will follow the bang-coast-bang acceleration command and zero angle line. The feedback loop of the CTP method is also enhanced with the LQR controller above. To make the acceleration output accessible for the actuator, the simulation is run with saturation of trolley acceleration and velocity.

As shown in Figure 4, the corresponding simulation results under external disturbance are presented for comparison, which contains the swing angles, trolley position, and the corresponding accelerations. In addition, the key control indicators are listed in Table 3, where T_f is the time after the trolley position error is less than 0.02m, and E_{θ_1} and E_{θ_2} are the largest angle errors after $25s$.

Table 3. Quantified comparable results

Method	T_f	θ_{1max}	θ_{2max}	E_{θ_1}	E_{θ_2}
Prop.	28.7	1.37	1.37	0.06	0.06
LQR	39.8	1.58	1.58	0.25	0.25
CTP	40.0	1.40	1.40	0.21	0.21

Based on the figure and table, it can be observed that all three methods are capable of executing position-changing commands. The proposed method uses the shortest time to achieve the desired trolley position and the angle reduction. The maximum value of the angle during the whole progress is also the smallest. In trolley positioning, both LQR and CTP suffer from overshoot and require additional time to settle at the desired position. Besides, LQR and CTP have lower angle reduction than the proposed method. At the same time, the angle errors of the proposed method at a certain time are smaller than the other two methods. In addition, the proposed acceleration of the motor is much smoother than LQR and CTP. The output curve would be easier to follow.

4 Conclusion

This paper introduces a trajectory planning method based on a position change request. A double pendulum system model is developed using the Lagrangian method, and a time-polynomial-based trajectory is derived. This trajectory minimizes the swing angles at the end state while simultaneously satisfying the actuator constraints (trolley jerk, acceleration, and velocity) for the entire progress. The controller exhibits remarkable performance in different simulated environments. Future research directions involve enhancing the degrees of freedom in the tower crane model to simulate real-world conditions better. It is important to note that incorporating trolley motion with jib rotation introduces additional nonlinear superposition terms, which may introduce inaccuracies during the linearization process. Additionally, to use 3D models in our future work, the integration of polynomial path planning for simultaneous control and obstacle avoidance could be explored. This comprehensive approach would offer a holistic solution for managing complex operational scenarios.

References

[1] Jongchul Song, Walter R Fagerlund, Carl T Haas, Clyde B Tatum, and Jorge A Vanegas. Considering prework on industrial projects. *Journal of construction engineering and management*, 131(6):723–733, 2005.

[2] Pei-Yuan Hsu, Panagiotis Angeloudis, and Marco Aurisicchio. Optimal logistics planning for modular construction using two-stage stochastic programming. *Automation in construction*, 94:47–61, 2018.

[3] Bon-Gang Hwang, Ming Shan, and Kit-Ying Looi. Key constraints and mitigation strategies for prefabricated prefinished volumetric construction. *Journal of cleaner production*, 183:183–193, 2018.

[4] Bingqing Zhao, Huimin Ouyang, and Makoto Iwasaki. Motion trajectory tracking and sway reduction for double-pendulum overhead cranes using improved adaptive control without velocity feedback. *IEEE/ASME Transactions on Mechatronics*, 27(5): 3648–3659, 2021.

[5] Šandor Ileš, Jadranko Matuško, and Mircea Lazar. Piece-wise ellipsoidal set-based model predictive

control of linear parameter varying systems with application to a tower crane. *Asian Journal of Control*, 23(3):1324–1339, 2021.

[6] Martin Böck and Andreas Kugi. Real-time nonlinear model predictive path-following control of a laboratory tower crane. *IEEE Transactions on Control Systems Technology*, 22(4):1461–1473, 2013.

[7] Qingxiang Wu, Xiaokai Wang, Lin Hua, and Minghui Xia. Modeling and nonlinear sliding mode controls of double pendulum cranes considering distributed mass beams, varying roped length and external disturbances. *Mechanical Systems and Signal Processing*, 158:107756, 2021.

[8] Menghua Zhang and Xingjian Jing. Model-free saturated pd-smc method for 4-dof tower crane systems. *IEEE Transactions on Industrial Electronics*, 69(10): 10270–10280, 2022.

[9] Ning Sun, Yongchun Fang, He Chen, Biao Lu, and Yiming Fu. Slew/translation positioning and swing suppression for 4-dof tower cranes with parametric uncertainties: Design and hardware experimentation. *IEEE Transactions on Industrial Electronics*, 63(10):6407–6418, 2016.

[10] Zheng Tian, Lili Yu, Huimin Ouyang, and Guangming Zhang. Sway and disturbance rejection control for varying rope tower cranes suffering from friction and unknown payload mass. *Nonlinear Dynamics*, 105(4):3149–3165, 2021.

[11] Menghua Zhang, Xingjian Jing, Weijie Huang, Quanli Lu, Jiyang Chen, and Zhenxue Chen. Robust fault accommodation approach for double-pendulum tower cranes via adaptive neural network-triggered control. *Nonlinear Dynamics*, pages 1–21, 2023.

[12] Menghua Zhang and Xingjian Jing. Adaptive neural network tracking control for double-pendulum tower crane systems with nonideal inputs. *IEEE Transactions on Systems, Man, and Cybernetics: Systems*, 52(4):2514–2530, 2021.

[13] Jiaohui Peng, Jie Huang, and William Singhose. Payload twisting dynamics and oscillation suppression of tower cranes during slewing motions. *Nonlinear Dynamics*, 98:1041–1048, 2019.

[14] Huimin Ouyang, Jinxin Hu, Guangming Zhang, Lei Mei, and Xin Deng. Decoupled linear model and s-shaped curve motion trajectory for load sway reduction control in overhead cranes with double-pendulum effect. *Proceedings of the Institution of Mechanical Engineers, Part C: Journal of Mechanical Engineering Science*, 233(10):3678–3689, 2019.

[15] Zhuoqing Liu, Tong Yang, Ning Sun, and Yongchun Fang. An antiswing trajectory planning method with state constraints for 4-dof tower cranes: design and experiments. *IEEE Access*, 7:62142–62151, 2019.

[16] Gang Li, Xin Ma, Zhi Li, and Yibin Li. Time-polynomial-based optimal trajectory planning for double-pendulum tower crane with full-state constraints and obstacle avoidance. *IEEE/ASME Transactions on Mechatronics*, 28(2):919–932, 2022.

[17] Huimin Ouyang, Zheng Tian, Lili Yu, and Guangming Zhang. Motion planning approach for payload swing reduction in tower cranes with double-pendulum effect. *Journal of the Franklin Institute*, 357(13):8299–8320, 2020.